European Journal of Pharmaceutics and Biopharmaceutics 75 (2010) 311–320

Contents lists available at ScienceDirect

European Journal of Pharmaceutics and Biopharmaceutics

journal homepage: www.elsevier.com/locate/ejpb

Research paper

Enhanced gene expression in epithelial cells transfected with amino acid-substituted gemini nanoparticles

Peng Yang [a], Jagbir Singh [b], Shawn Wettig [c], Marianna Foldvari [c], Ronald E. Verrall [a], Ildiko Badea [b,*]

[a] Department of Chemistry, University of Saskatchewan, Saskatoon, Canada
[b] Drug Design and Discovery Research Group, College of Pharmacy and Nutrition, University of Saskatchewan, Saskatoon, Canada
[c] School of Pharmacy, University of Waterloo, Waterloo, Canada

ARTICLE INFO

Article history:
Received 30 October 2009
Accepted in revised form 16 April 2010
Available online 22 April 2010

Keywords:
Gene therapy
In vitro transfection
Non-viral
Epithelial cells
Nanoparticles
Delivery efficiency

ABSTRACT

Gemini surfactants are versatile gene delivery agents because of their ability to bind and compact DNA and their low cellular toxicity. Through modification of the alkyl tail length and the chemical nature of the spacer, new compounds can be generated with the potential to improve the efficiency of gene delivery. Amino acid (glycine and lysine) and dipeptide (glycyl-lysine and lysyl-lysine) substituted spacers of gemini surfactants were synthesized, and their efficiency of gene delivery was assessed in epithelial cells for topical cutaneous and mucosal applications.

Three different epithelial cell lines, COS-7, PAM212 and Sf 1Ep cells, were transfected with plasmid DNA encoding for interferon gamma and green fluorescent protein complexed with the amino acid-substituted gemini compounds in the presence of 1,2 dioleyl-*sn*-glycero-phosphatidyl-ethanolamine as a helper lipid. Gene expression was quantified by ELISA. Size, zeta potential and circular dichroism measurements were used to characterize the plasmid–gemini (PG) and plasmid–gemini surfactant–helper lipid (PGL) complexes.

Gene expression was found to increase up to 72 h and then declined by the 7th day. In general, the glycine-substituted surfactant showed consistently high gene expression in all three cell lines. Results of physicochemical and spectroscopic studies of the complexes indicate that substitution of the gemini spacer does not interfere with compaction of the DNA.

The superior performance of these spacer-substituted gemini surfactants might be attributed to their better biocompatibility compared to the surfactants possessing unsubstituted spacers.

1. Introduction

Topical gene delivery is an important approach in the quest to find treatment or cure for a multitude of genetic and acquired disorders, such as scleroderma, epidermolysis bullosa, cystic fibrosis and others. To correct the imbalances created by a missing or incorrect gene, efficient non-invasive gene delivery systems should be employed. Interferon gamma (IFN-γ) is a secreted cytokine with immunomodulatory, antiviral, antifibrotic and antitumour activity. Based on these properties, its therapeutic potential in conditions such as scleroderma [1], atopic dermatitis [2] and post-operatory fibrosis [3] have been discussed, and delivery of IFN-γ gene into epidermal skin and mucosal epithelial tissue can be considered for these applications. Gemini surfactants, *N*,*N*-bis(dimethylalkyl)-α,ω-alkanediammonium halide derivatives (Fig. 1) [4], have been shown to be versatile vectors for non-viral gene delivery [5–8]. This stems from the fact that there are many possibilities, through chemical modification of the alkyl tails and the spacer group of these compounds, to modulate their physicochemical behaviour in a way that can enhance the efficiency of gene transfer. For example, modification of the length, degree of unsaturation and substitution of different functional groups in the spacer and alkyl tails can provide opportunities to tailor their chemical structure for specific needs [9,10].

Cationic gemini surfactants are capable of binding DNA [11] and have several advantages compared to classic monovalent surfactants: lower cellular toxicity [7], lower critical micelle concentration (cmc), generally one or two orders of magnitude higher efficiency in reducing surface tension and greater tendency to self-assemble [12]. The higher order assembly of the gemini surfactants depends on the shape of the molecule (i.e., nature of the tail and spacer) and ranges from micellar to inverted micellar or bilayer structures. In the presence of the DNA, these supramolecular particles become more complex, resulting in polymorphic phase behaviour with the appearance of inverted micellar and

* Corresponding author. College of Pharmacy and Nutrition, University of Saskatchewan, 110 Science Place, Thorvaldson Building, Room G22, Saskatoon, Saskatchewan, Canada S7N 5C9. Tel.: +1 306 966 6349.
E-mail address: ildiko.badea@usask.ca (I. Badea).

0939-6411/$ - see front matter © 2010 Elsevier B.V. All rights reserved.
doi:10.1016/j.ejpb.2010.04.007

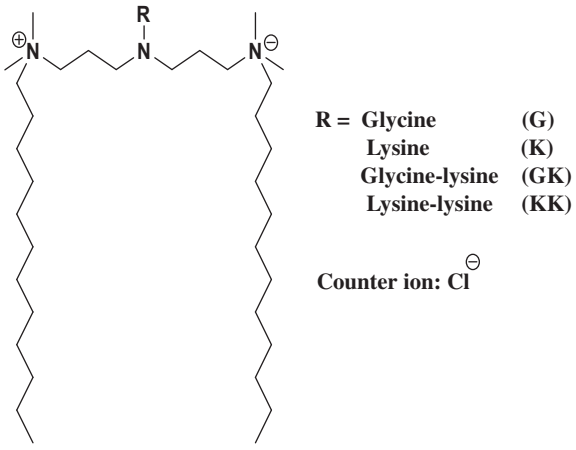

Fig. 1. General structure of gemini surfactants. The two hydrophobic alkyl chains (tail) with charged head groups (ion) are connected with a carbon spacer [4].

cubic structures [13]. To be efficient transfection agents, they have to fulfil several criteria: ability to bind DNA and create complexes of a certain size and morphology, the vector–plasmid complexes must retain an overall positive surface charge so as to facilitate interaction with the negative cell surface and enhance cellular uptake (in the absence of specific targeting), induce changes in the DNA structure favourable for efficient delivery, protect the genetic material against intracellular degradation, have the ability to undergo polymorphic phase changes and undergo facile release of the plasmid once inside the cell to effect protein expression. Gemini surfactants with C3–C12 alkyl spacers are able to compact the DNA into 100–200 nm particles with positive surface charge [5], which enables interaction with the cell surface and endocytosis. The transfection efficiency of these agents depends on the spacer length, the 3-carbon spacer (12-3-12) being the most efficient. CD spectra of the plasmid–gemini surfactant complexes have previously been discussed in terms of the formation of highly compact Ψ^- DNA [5]. Addition of a helper lipid, 1,2 dioleyl-*sn*-glycero-phosphatidyl-ethanolamine (DOPE), induces polymorphic phase behaviour [13], which correlates with increased transfection efficiency [5]. Cellular toxicity of the transfection complexes was significantly lower compared to the commercial Lipofectamine Plus [5]. Substitution of the alkyl spacer with pH-sensitive imino groups increases the transfection efficiency of the gemini surfactants [8]. The 1,9-bis(dodecyl)-1,1,9,9-tetramethyl-5-imino-1,9-nonanediammonium dibromide surfactant (12-7NH-12) transfected cells at a ninefold higher level compared to the alkyl spacer derivatives. This improvement was attributed to its pH sensitivity and ability to form multiple phases, which enable membrane fusion and release of the DNA in the cells [8].

We report here the results of a study focusing on the modification of this derivative by chemically coupling amino acid moieties to the imino spacer so as to further increase and prolong gene expression. It has been shown that small molecular weight pep-

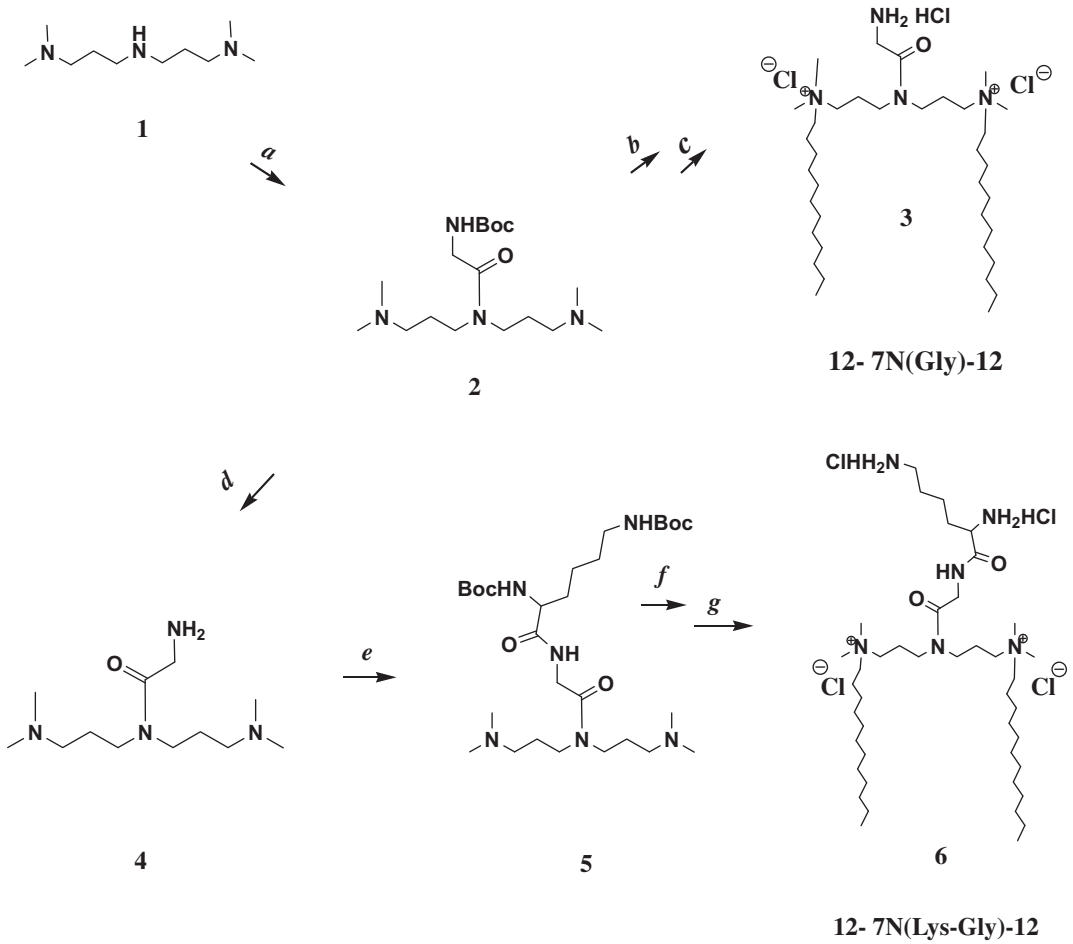

Fig. 2. Synthetic scheme #1: (a) Boc-glycine, EEDQ, $CHCl_3$; (b) 1-bromododecane, MeCN; (c) (i) TFA, $CHCl_3$; (ii) Cl^- ion exchange; (d) (i) TFA, $CHCl_3$; (ii) NaOH, EtOH; (e) Boc-Lys(Boc)-OH,EEDQ,$CHCl_3$; (f) 1-bromododecane, MeCN; (g) (i) TFA, $CHCl_3$; (ii) Cl^- ion exchange.

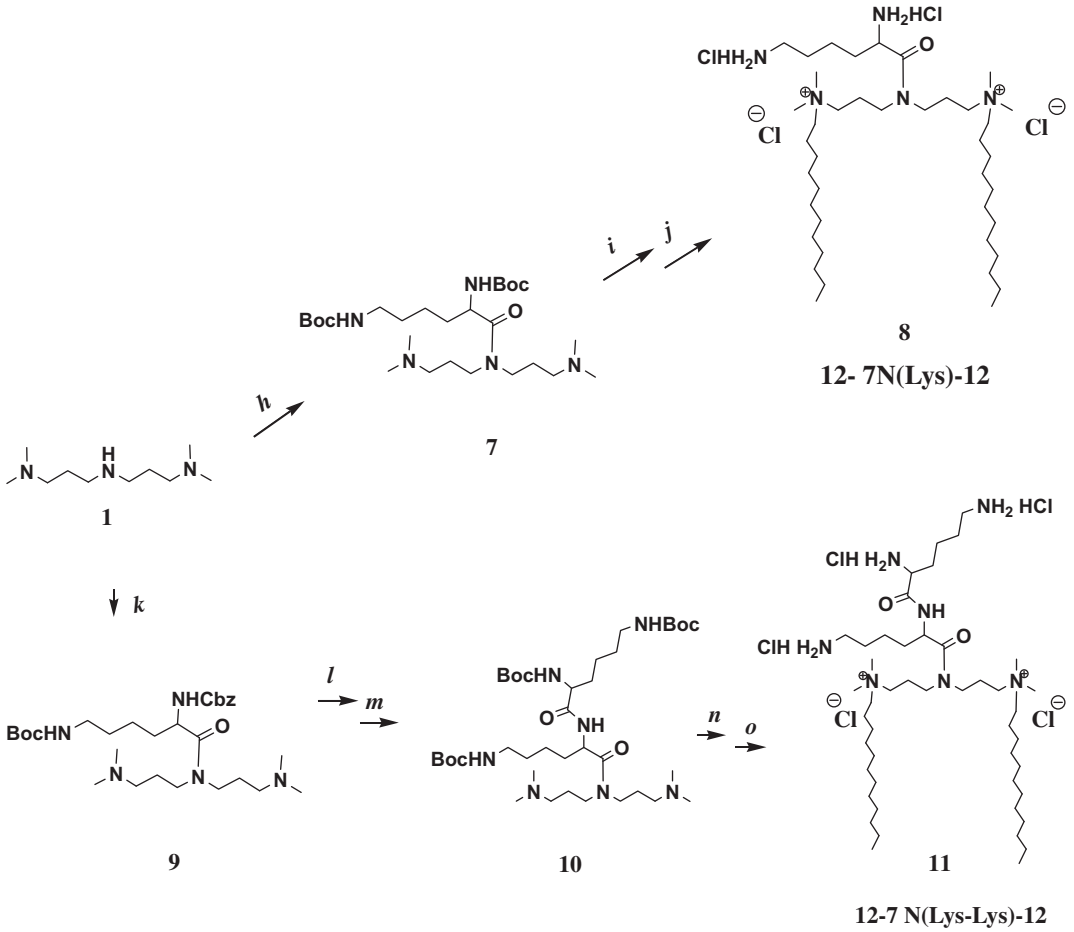

Fig. 3. Synthetic scheme #2: (h) Boc-Lys(Boc)-OH, EEDQ, $CHCl_3$; (f) 1-bromododecane, MeCN; (g) (i) TFA, $CHCl_3$; (ii) Cl^- ion exchange; (k) Cbz-Lys(Boc)-OH, EEDQ,$CHCl_3$; (l) $HCOONH_4$, 10% Pd/C; (m) Boc-Lys(Boc)-OH, EEDQ,$CHCl_3$; (n) 1-bromododecane, MeCN; (o) (i) TFA, $CHCl_3$; (ii) Cl^- ion exchange.

tides such as arginine-rich protamine fragments are able to bind and condense DNA into 100-nm particles. Transfection of cells resulted in prolonged gene expression for up to 12 days [14]. We hypothesized that an additive effect could be achieved by coupling the highly efficient imino-substituted spacer of a gemini surfactant with amino acid/dipeptide residues.

2. Materials and methods

2.1. Synthesis of amino acid/dipeptide-substituted gemini surfactants

Boc-lys-OH, Boc-lys(Cbz)-OH and 3,3′-iminobis (*N,N*-dimethylpropylamine) were purchased from Sigma–Aldrich; Boc-gly-OH and EEDQ were purchased from Alfa Aesar. All solvents used were of the highest grade and purchased from Sigma–Aldrich. These chemicals were used without further purification. ^{1}H NMR spectra were recorded in either $CDCl_3$ or CD_3OD using a 500 MHz Bruker spectrometer, and mass spectra were obtained using a QSTAR XL MS/MS System.

2.2. Specific conductance – determination of the critical micelle concentrations

Specific conductivities were measured as previously described using a Wayne-Kerr precision component analyzer (Model 6425) operating at 1.5 kHz, with a Tacussel electrode having a cell constant of 1.11 cm^{-1} [15]. Experimental temperatures were maintained at 25 ± 0.05 °C using a Haake (Model F3) circulating water bath. The specific conductance was measured after each addition of an aqueous solution of concentrated surfactant into water under a nitrogen atmosphere, allowing for the solution to equilibrate.

2.3. Preparation of the gene delivery systems

The pGT·IFN-GFP plasmid was used for the transfection experiments. The murine interferon gamma (IFN-γ) and green fluorescent protein (GFP) genes were inserted into the pGT backbone as a bicistronic system [5]. Transfection agents of plasmid/gemini surfactant (PG) complexes and plasmid/gemini surfactant/helper lipid (PGL) particles were prepared as previously described [5]. The plasmid:gemini surfactant charge ratio was 1:10. DOPE was used as a helper lipid.

2.4. Transfection of COS-7, PAM212 and Sf 1Ep cells using amino acid/dipeptide-substituted gemini surfactants and DOPE

COS-7 African green monkey kidney fibroblasts (ATCC, CRL-1651), PAM212 murine keratinocytes (kindly provided by Dr. S. Yuspa, NCI) and Sf 1Ep cottontail rabbit epithelial cells (ATCC, CCL-68) were seeded on Falcon 96-well tissue culture plates (BD, Mississauga, ON) at a density of 2×10^5 cells/well. Three plates were seeded with each cell line at the same passage number after initiation of the cultures. Transfection experiments were carried out using 100 ng plasmid DNA/well. Supernatants were collected every 24 h and replaced with fresh cell culture medium. The results are the average of three plates of triplicate wells.

2.4.1. ELISA

ELISA was used to detect IFN-γ secreted into the supernatant and was performed according to the BD Pharmingen protocol. Protein concentration was calculated from a standard curve using recombinant IFN-γ.

2.5. Size and zeta potential measurements

Size and zeta potential measurements of PG and PGL complexes, prepared at 1:10 plasmid:gemini surfactant charge ratio, the same as for the transfection experiments, were carried out using a Zetasizer Nano ZS instrument (Malvern Instruments, Worcestershire, UK). The results reported are the average of triplicate measurements on a % volume basis. Size measurements of gemini compounds at two concentrations above the cmc were also carried out on % volume basis.

2.6. Circular dichroism

PG and PGL complexes were prepared at the same charge and molar ratio as for transfection experiments, using 20 μg/mL plasmid DNA. Spectra were recorded using *Π**180 instrument (Applied Photo Physics, UK), with 2-nm slit under a N_2 atmosphere.

2.7. Statistics

Results are expressed as the mean of $n \geqslant 3 \pm$ standard deviation. One way analysis of variance (ANOVA) and Bonferroni post hoc tests were used for statistical analyses (SPSS version 16.0). Significant differences were considered at $p < 0.05$ level.

3. Results

3.1. Synthesis of amino acid/dipeptide-substituted gemini surfactants

3.1.1. General synthetic procedure

The coupling reactions between 3,3′-iminobis (*N,N*-dimethylpropylamine) and protected amino acids were carried out in the presence of EEDQ, and the intermediates were purified by separation on a silica column [16]. Subsequently, quaternization was carried out as previously described [17] followed by de-protection of the amino acids to give the target compounds.

3.1.2. Synthesis of 12-7N(Gly)-12 (**3**) and 12-7N(Lys-Gly)-12 (**6**) (Fig. 2)

Step a: Synthesis of N-2-(tert-butyloxycarbonyl) amino-*N,N*-bis[3-(dimethylamino)propyl]-acetamide (**2**).

Three grams (17.1 mmol) of Boc-glycine and 6.3 g (25.7 mmol) of N-ethoxycarbonyl-2-ethoxy-1,2-dihydroquinoline (EEDQ) were dissolved in 30 mL of $CHCl_3$ and stirred at room temperature for 10 min. Then, 3.85 g (20.6 mmol) of 3,3′-iminobis (*N,N*-dimethylpropylamine) (**1**) dissolved in 10 mL of $CHCl_3$ was added, gradually, to the solution, and the reactants were stirred for an additional 10 min upon completion of the addition of amine. Finally, the solution was refluxed for 2 days under a N_2 atmosphere.

Upon completion of the reaction, monitored by TLC, the solvent was removed under vacuum, and the product was separated by column chromatography (230–400 mesh silica gel) eluting with $CHCl_3$/MeOH (8:2, v/v) to obtain 4.75 g of colourless, oil-like product (**2**) (yield 81%). ^{1}H NMR ($CDCl_3$) δ/ppm: 5.55 (brs, 1H), 3.99–3.96 (m, 2H), 3.40–3.22 (m, 4H), 2.35–2.16 (m, 16H), 1.76–1.67 (m, 4H), 1.43 (s, 9H); ESI-MS *m/z*: 345.2968 [M^+].

Step b: Synthesis of 1,9-bis(dodecyl)-1,1,9,9-tetramethyl-5-(N′-Boc-glycyl)amino-1,9-nonanediammonium dibromide.

One gram (2.9 mmol) of (**2**) and 3.0 g (12 mmol) of 1-bromododecane were dissolved in 20 mL of dry MeCN, and the reaction mixture was refluxed at 60 °C for 3 days under a N_2 atmosphere. The solvent was removed under vacuum, and a large excess of diethyl ether was added to the residue and left overnight to make sure that the fine, suspended solid would settle. The organic phase was removed under vacuum. This process was repeated four times to ensure that all of the 1-bromododecane had been removed. The white solid was collected and dried under vacuum to obtain 1.85 g of product (yield, 76%). ^{1}H NMR($CDCl_3$) δ/ppm, 5.59 (brs, 1H), 4.11–3.99 (m, 2H), 3.81–3.59 (m, 6H), 2.55–3.41 (m, 4H), 3.39–3.25(s, 14H), 2.34 (brs, 2H), 2.18 (brs, 2H), 1.69 (brs, 4H), 1.38 (s, 9H), 1.34–1.14 (m, 36H), 0.83 (brs, 6H); ESI-MS *m/z*: 341.3349 $[M]^{2+}/2$.

Step c: Synthesis of 12-7N(Gly)-12 (**3**).

(i) De-protection of (**3**) was carried out by dissolving 1.0 g in 30 mL of $CHCl_3$ and stirring at 0 °C for 30 min followed by addition of 10 mL of TFA, drop-wise. The solution was removed from the ice bath, and the reaction was continued at room temperature for 24 h. The solvent was removed under vacuum.

(ii) The bromide salt of (**3**) was converted to chloride using Amberlite IRA-400(Cl) ion exchange resin. The chloride salt was then dissolved in 50 mL of methanol, and 3 g of charcoal was added. The mixture was refluxed for 30 min, cooled to room temperature and stirred overnight. The charcoal was removed by filtration, and the solution was reduced to a small volume, and the product was salted-out with acetone. This was repeated several times to yield 0.2 g of compound (**3**), 1,9-bis(dodecyl)-1,1,9,9-tetramethyl-5-glycylamino-1,9-nonanediammonium dichloride, hydrochloride salt (yield, 24%). ^{1}H NMR (CD_3OD) δ/ppm, 4.11 (brs, 2H), 3.75–3.23 (m, 14H), 3.24–3.06 (m, 12H), 2.31–2.02 (m, 4H), 1.83 (brs, 4H), 1.51–1.22 (m, 36H), 0.92 (brs, 6H); ESI-MS *m/z*: 291.3090 $[M]^{2+}/2$.

Step d: Synthesis of N-2-amino-*N,N*-bis[3-(dimethylamino)-propyl]-acetamide (**4**).

(i) De-protection of (**2**) followed the procedure outlined in step c (i) to give a white solid. ^{1}H NMR (CD_3OD) δ/ppm, 4.05 (brs, 2H), 3.49–3.33 (m, 4H), 3.20–3.07 (m, 4H), 2.87 (s, 6H), 2.85 (brs, 8H), 2.09–1.91 (m, 4H); ESI-MS *m/z*: 245.2341 $[M+H]^+$.

(ii) The white solid was dissolved in 10 mL of EtOH, 0.2 g of KOH pellets was added, and the mixture stirred at 0 °C for 1 h. Afterwards, the EtOH was removed under vacuum, and the residue was transferred to a separatory funnel containing a mixture of $CHCl_3/H_2O$, 150 mL/20 mL. The organic phase was collected, dried over Na_2SO_4, and the solvent was removed under vacuum to obtain 0.3 g of oil-like (**4**) (yield, 45%).

Step e: Synthesis of *N,N*-bis[3-(dimethylamino)propyl]-[N′-(N^{α}-N^{ε}-di-Boc-L-lysyl)]-glycinamide (**5**).

The coupling of intermediate (**4**) and Boc-lys (Boc)-OH followed the procedure outlined in step a to give 0.51 g of (**5**) (yield, 74%). ^{1}H NMR ($CDCl_3$) δ/ppm, 7.09 (s, 1H), 5.39 (s, 1H), 4.94 (s, 1H), 4.20–3.89 (m, 3H), 3.36–3.12 (m, 4H), 2.97 (brs, 2H), 2.24–2.12 (m, 4H), 2.11–2.05 (brs, 12H), 1.80–1.21 (m, 28H); ESI-MS *m/z*: 573.4360 $[M+H]^+$.

Step f: Synthesis of 1,9-bis(dodecyl)-1,1,9,9-tetramethyl-5-[N′-(N$^{\alpha}$-N$^{\varepsilon}$-di-Boc-L-lysyl)glycyl]amino-1,9-nonanediammonium dibromide.

The synthesis and purification of this intermediate followed the procedure outlined in step b (yield 88%).

^{1}H NMR ($CDCl_3$) δ/ppm, 7.87 (s, 1H), 5.42 (s, 1H), 4.92 (s, 1H), 4.24–4.06 (m, 3H), 3.85–3.51 (m, 8H), 3.50–3.20 (m, 16H), 3.02 (brs, 2H), 2.44–2.09 (m, 4H), 1.85–1.57 (m, 6H), 1.41–1.13 (m, 58H), 0.83–0.81 (t, 6H, J = 5.0 Hz).

Step g: Synthesis of 12-7N(Lys-Gly)-12 (**6**).

The synthesis and purification of 12-7N(Lys-Gly)-12 (**6**) followed the procedure outlined in step c (yield 30%). ^{1}H NMR ($CDCl_3$) δ/ppm, 4.26 (brs, 2H), 4.07 (brs, 1H), 3.75–2.88 (m, 31H), 2.33–1.18 (m, 50H), 0.92 (brs, 6H); ESI-MS m/z: 355.3559 $[M]^{2+}/2$.

*3.1.3. Synthesis of 12-7N(Lys)-12 (**8**) and 12-7N(Lys-Lys)-12 (**11**) (Fig. 3)*

Step h: Synthesis of *N,N-bis[3-(dimethylamino)propyl]-N$^{\alpha}$*-N$^{\varepsilon}$-di-Boc-L-lysinamide (**7**).

The synthesis and purification of (**7**) followed the procedure outlined in step a (yield 83%).^{1}H NMR ($CDCl_3$) δ/ppm, 5.38–5.31 (m, 1H), 5.15 (brs, 1H), 4.35 (brs, 1H), 4.0 (brs, 1H), 3.36–3.05 (m, 2H), 2.99–2.79 (m, 3H), 2.08–2.01 (m, 4H), 1.98 (brs, 12H), 1.62–1.29 (m, 7H), 1.23–1.17 (brs, 21H); ESI-MS m/z: 516.4095 $[M+1]^+$.

Step i: Synthesis of 1,9-bis(dodecyl)-1,1,9,9-tetramethyl-5-(N$^{\alpha}$-N$^{\varepsilon}$-di-Boc-L-lysyl)amino-1,9-nonanediammonium dibromide.

The synthesis and purification of this intermediate followed the procedure outlined in step b (yield 69%). ^{1}H NMR ($CDCl_3$) δ/ppm, 5.33 (brs, 1H), 4.96 (brs, 1H), 4.42 (brs, 1H), 3.95–3.26 (m, 24H), 3.08 (brs, 2H), 2.49–2.17 (m, 4H), 1.90–1.18 (m, 64H), 0.87–0.85 (t, 6H, J = 5.0 Hz); ESI-MS m/z: 426.8980 $[M]^{2+}/2$.

Step j: Synthesis of 12-7N(Lys)-12 (**8**).

The synthesis and purification of 12-7N(Lys)-12 (**8**) (1,9-bis(dodecyl)-1,1,9,9-tetramethyl-5-(L-lysyl)amino-1,9-nonanediammonium dichloride, dihydrochloride salt) was carried out according to step c (yield 35%). ^{1}H NMR ($CDCl_3$) δ/ppm, 4.53 (brs, 1H), 3.71–3.36 (m, 16H), 3.27–3.10 (m, 12H), 3.00 (brs, 2H), 2.32–1.51 (m, 14H), 1.51–1.25 (m, 36H), 0.92 (brs, 6H); ESI-MS m/z: 326.8460 $[M]^{2+}/2$.

Step k: Synthesis of *N,N*-bis[3-(dimethylamino)propyl]-N$^{\varepsilon}$-Boc-N$^{\alpha}$-Cbz-L-lysinamide (**9**).

The synthesis and purification of this intermediate followed the procedure outlined in step a (yield, 76%). ^{1}H NMR ($CDCl_3$) δ/ppm, 7.41–7.30 (brs, 5H), 5.68 (brs, 1H), 5.08 (brs, 2H), 4.82 (brs, 1H), 4.65 (brs, 1H), 3.63–2.99 (m, 6H), 2.36–2.15 (m, 16H), 1.85–1.34 (m, 19H); ESI-MS m/z: 550.3954 $[M+H]^+$.

Step l: Synthesis of *N,N*-bis[3-(dimethylamino)propyl]-N$^{\varepsilon}$-Boc-L-lysinamide.

One gram (1.8 mmol) of (**9**) and 0.4 g (6.3 mmol) of $HCOONH_4$ were dissolved in 10 mL of anhydrous MeOH and stirred for 10 min at room temperature under a N_2 atmosphere. Then, 0.3 g of 10% Pd/C was added, gradually, over 30 min, and the reaction was continued for a further 24 h at room temperature. The catalyst was removed by filtration, and the MeOH was removed under vacuum, followed by transfer of the residue to a separatory funnel containing a 2-phase system of $CHCl_3$ and 1 wt.% Na_2CO_3 in water. The organic phase was collected and washed, twice, with water and dried over Na_2SO_4. The $CHCl_3$ was removed under vacuum to obtain 0.31 g product (isolated yield, 42%). ^{1}H NMR ($CDCl_3$) δ/ppm, 3.93 (brs, 1H), 3.63–3.43 (m, 2H), 3.42–3.23 (m, 3H), 3.06 (brs, 2H), 2.59 (brs, 2H), 2.48 (brs, 8H), 2.37 (s, 6H), 1.95–1.33 (m, 19H); ESI-MS m/z: 416.3598 $[M+H]^+$.

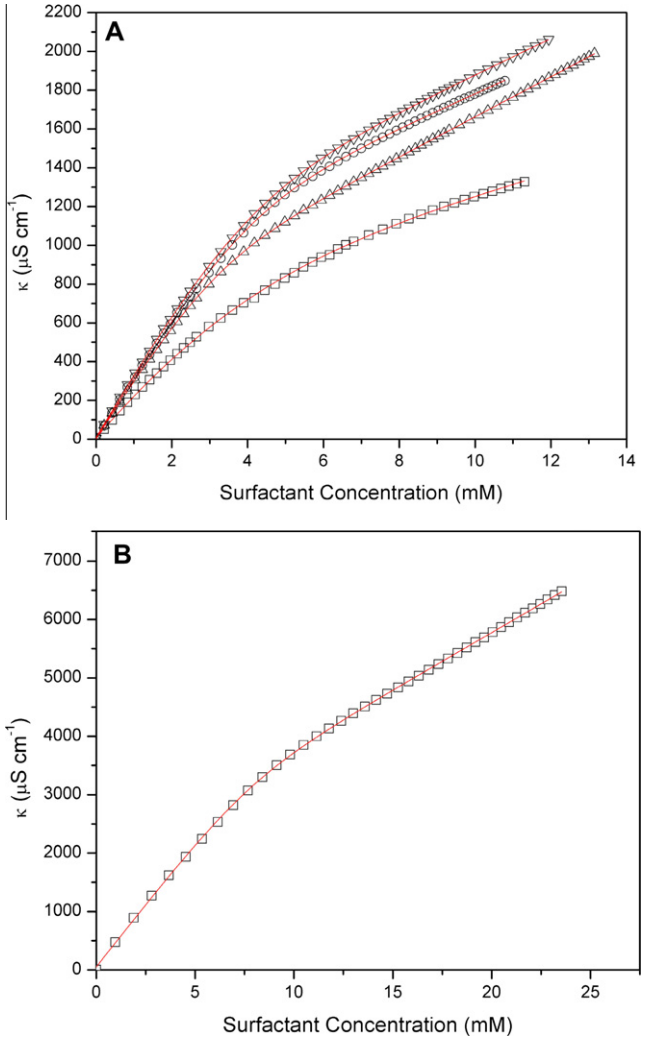

Fig. 4. Specific conductivities of the amino acid-modified gemini surfactants: (A) 12-7NH-12·2Cl □, 12-NK-12 ○, 12-NG-12 Δ, 12-7NKG-12 ▽; (B) 12-NKK-12. Lines represent fit to Eq. (1). (For interpretation of the references to colour in this figure legend, the reader is referred to the web version of this article.)

Step m: Synthesis of *N,N*-bis[3-(dimethylamino)propyl]-N$^{\alpha}$-(N$^{\alpha'}$-N$^{\varepsilon'}$-di-Boc-L-lysyl)-N$^{\varepsilon}$-Boc-L-lysinamide (**10**).

The synthesis and purification of (**10**) followed the procedure outlined in step a (yield 83%).^{1}H NMR ($CDCl_3$) δ/ppm, 6.89–6.78 (m, 1H), 5.22 (brs, 1H), 4.98–4.85 (m, 3H), 4.06 (brs, 1H), 3.60–3.50 (m, 1H), 3.47–3.38 (m, 1H), 3.33–3.24 (m, 1H), 3.18–3.03 (m, 5H), 2.31–2.22 (m, 4H), 2.20 (brs, 12H), 1.84–1.40 (m, 39H), 1.38–1.29 (m, 4H); ESI-MS m/z: 744.5591 $[M+H]^+$.

Step n: Synthesis of 1,9-bis(dodecyl)-1,1,9,9-tetramethyl-5-[N$^{\alpha}$-(N$^{\alpha'}$-N$^{\varepsilon'}$-di-Boc-L-lysyl)-N$^{\varepsilon}$-Boc-L-lysyl)]amino-1,9-nonanediammonium dibromide.

Table 1
Critical micelle concentration fitting parameters.

Surfactant	A_1 (μS cm^{-1} mM^{-1})	A_2 (μS cm^{-1} mM^{-1})	d (mM)	cmc (mM)	α[a]
12-7NG-12	313 ± 2	103.2 ± 0.2	0.97 ± 0.01	2.94 ± 0.03	0.330 ± 0.002
12-7NK-12	320 ± 3	87.8 ± 0.7	1.16 ± 0.03	3.81 ± 0.03	0.274 ± 0.003
12-7NGK-12	340 ± 2	93.3 ± 0.5	1.32 ± 0.02	3.72 ± 0.03	0.274 ± 0.002
12-7NKK-12	432 ± 7	196 ± 1	1.8 ± 0.1	7.6 ± 0.2	0.454 ± 0.008
12-7NH-12·2Cl$^-$	290 ± 30	55 ± 4	2.4 ± 0.3	2.1 ± 0.6	0.19 ± 0.02
12-7NH-12·2Br$^-$[b]	196 ± 7	49 ± 5	0.54 ± 0.5	1.24 ± 0.06	0.25 ± 0.05

[a] Equal to A_2/A_1.
[b] Data from [8].

The synthesis and purification of this intermediate followed the procedure outlined in step b (yield 85%). ^{1}H NMR ($CDCl_3$) δ/ppm, 7.45 (brs, 1H), 5.63 (brs, 1H), 5.04 (brs, 1H), 4.86 (brs, 1H), 4.70 (brs, 1H), 4.01 (brs, 1H), 3.87–3.36 (m, 12H), 3.31 (brs, 12H), 3.08 (brs, 4H), 2.61–2.11 (m, 4H), 1.90–1.20 (m, 79H), 0.88–0.86 (t, 6H, J = 5.0 Hz); ESI-MS m/z: 540.9698 $[M]^{2+}/2$.

Step o: Synthesis of 12-7N(Lys-Lys)-12 (**11**).

The synthesis and purification of 12-7N(Lys-Lys)-12 (**11**) (1,9-bis(dodecyl)-1,1,9,9-tetramethyl-5-[N$^{\alpha}$-(L-lysyl)-L-lysyl)]amino-1,9-nonanediammonium dichloride, trihydrochloride salt) was carried out according to the procedure followed in step c (yield 38%). ^{1}H NMR ($CDCl_3$) δ/ppm, 4.73 (brs, 1H), 4.07 (brs, 1H), 3.93 (brs, 1H), 3.81–3.31 (m, 18H), 3.22–3.11 (m, 12H), 3.07–2.97 (m, 4H), 2.44–1.26 (m, 56H), 0.93–0.91 (t, 6H, J = 5.0 Hz); ESI-MS m/z: 390.8914 $[M]^{2+}/2$.

3.2. Physiochemical characterization of amino acid/dipeptide-substituted gemini compounds

3.2.1. Critical micelle concentration

Specific conductance vs. concentration graphs for the amino acid-substituted gemini surfactants are shown in Fig. 4. Fitting parameters, including the cmc and degree of micelle ionization (α) for the amino acid-substituted gemini surfactants, are reported in Table 1. Critical micelle concentrations were determined from a fit of the specific conductivity data according to the method of Carpena et al. [18], using the relation:

$$\kappa = \kappa_0 + A_1 c + d(A_2 - A_1)\ln\left(\frac{1 + e^{(c\text{-cmc})/d}}{1 - e^{-\text{cmc}/d}}\right) \quad (1)$$

where A_1 and A_2 are the pre-cmc and post-cmc slopes of the κ vs. concentration curve and d is the width of the cmc transition region. Initial estimates of A_1 and A_2 were obtained from the pre-cmc and post-cmc slopes, respectively. Initial values of the cmc were obtained from the approximate breakpoints in the specific conductance vs. concentration curves, and the initial estimate of d was obtained from the approximate spacing between data points. The initial specific conductance value, κ_0, was obtained from the reading at zero concentration.

Table 2
Aggregate size of the amino acid/dipeptide-substituted gemini surfactants above cmc.

Surfactant	Concentration (mM)	Diameter (nm)
12-7NG-12	6	3.67
	10	3.22
12-7NK-12	6	5.68
	10	3.94
12-7NGK-12	6	5.85
	10	3.54
12-7NKK-12	12	4.21
	20	3.73

3.2.2. Hydrodynamic size of self-aggregates

Estimates of the hydrodynamic diameters (Table 2) of the self-aggregates of these gemini compounds (in the absence of DNA) were obtained from DLS measurements made at two concentrations above the cmc. The sizes of all the amino acid-substituted gemini were found to decrease as the surfactant concentration above the cmc was increased.

3.3. Transfection of cells with amino acid/dipeptide-substituted gemini surfactants

3.3.1. Transfection of COS 7 cells

The screening of the new derivatives was carried out using the generally easy to transfect COS7 cell line. As controls, the 12-7NH-12 parent gemini surfactant and Lipofectamine Plus were used. All transfections were carried out in the presence of helper lipid, DOPE. Gene expression increased significantly ($p < 0.001$) in all PGL complexes and Lipofectamine Plus from 24 to 72 h (Fig. 5). Some gene expression was observed after 1 week, but it was

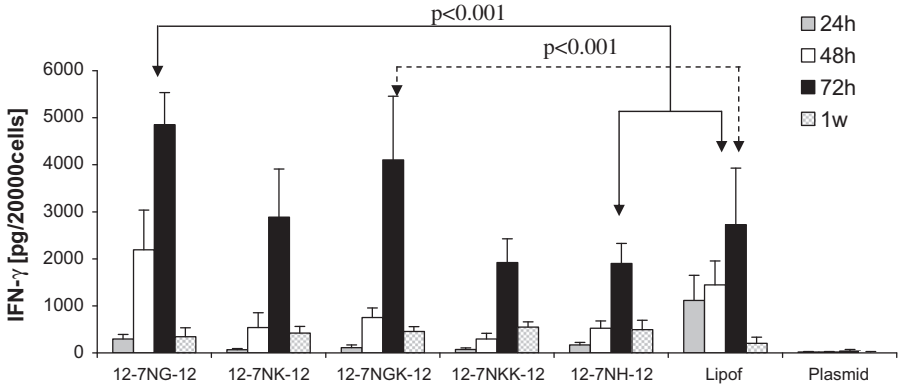

Fig. 5. Gene expression in COS7 cells transfected with PGL complexes. Triplicate wells of each sample were loaded on three different plates. The results are expressed as mean of the plates (n = 3). Bars represent standard deviation.

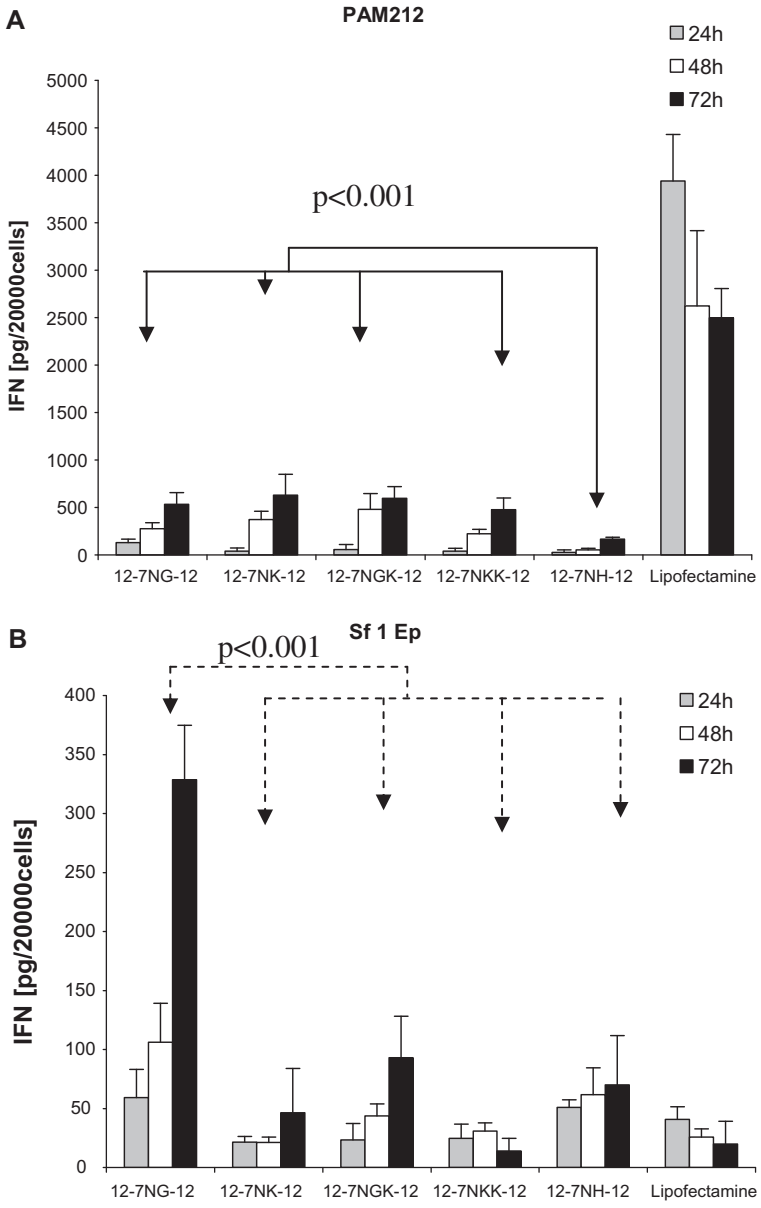

Fig. 6. Gene expression in PAM212 (A) and Sf 1Ep (B) cells transfected with PGL complexes. Triplicate wells of each sample were loaded on three different plates. The results are expressed as mean of the plates ($n = 3$). Bars represent standard deviation.

Table 3
Size and zeta potential measurements. Values are average of four measurements ± STD. Polydispersity (PDI) index is indicated for the size measurements as average of four measurements ± STD in brackets.

PGL	Size (nm) (PDI)	Zeta potential (mV)
P/12-7NG-12/DOPE	116.3 ± 1.3 (0.252 ± 0.008)	32.6 ± 1.8
P/12-7NK-12/DOPE	112.7 ± 1.7 (0.265 ± 0.006)	28.6 ± 3.6
P/12-7NGK-12/DOPE	117.3 ± 0.6 (0.232 ± 0.012)	34.5 ± 5.6
P/12-7NKK-12/DOPE	105.3 ± 0.4 (0.245 ± 0.008)	31.3 ± 4.0
P/12-7NH-12/DOPE	133 ± 2.8 (0.279 ± 0.006)	24.9 ± 3.4
P/DOPE	98.2 ± 0.3 (0.224 ± 0.008)	−32.7 ± 0.6

drastically diminished compared to the previous time point. At 72 h, the highest level of gene expression was measured in the cells transfected with the 12-7NG-12 PGL, 4.8 ± 0.6 ng IFN-γ/2 × 10^5 cells, significantly higher compared to the 12-7NH-12 PGL, 1.9 ± 0.4 ng IFN-γ/2 × 10^5 cells, ($p < 0.001$) and Lipofectamine Plus, 2.7 ± 1.2 ng IFN-γ/2 × 10^5 cells, ($p < 0.001$). IFN-γ levels were also significantly higher in the supernatants collected from cells transfected with the 12-7NGK-12 PGL, 4.1 ± 1.4 ng IFN-γ/2 × 10^5 cells, compared to Lipofectamine Plus ($p = 0.001$). The other two amino acid-substituted gemini surfactants, 12-7NK-12 and 12-7NKK-12, performed similarly to the controls. Minimal gene expression was observed in the cells transfected with the plasmid and DOPE, in the absence of gemini surfactant.

3.3.2. Transfection of PAM212 and Sf 1Ep cells

The amino acid-substituted gemini surfactants are designed for topical (cutaneous and mucosal) gene delivery. Two different cell lines were transfected, the previously used PAM 212 keratinocytes and the Sf 1Ep epithelial cells (Fig. 6). Similar to COS7 cells, gene expression in the PAM212 cell line increased significantly in time ($p < 0.001$). However, there was little or no protein detected after 1 week (results not shown). In PAM212 cells, the highest gene expression was observed with the 12-7NK-12 at 72 h, 631 ± 218 pg IFN-γ/2 × 10^5 cells. There was no significant

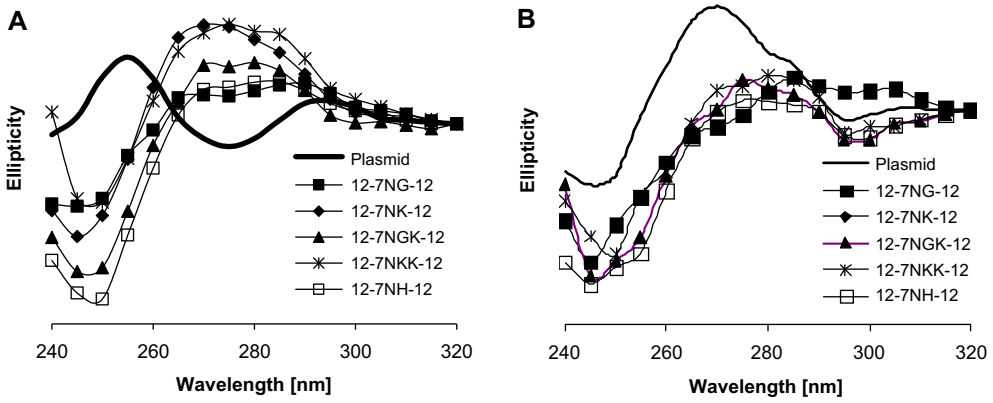

Fig. 7. CD spectra of the PG complexes (A) and the PGL particles (B). Values are average of three measurements.

difference among the substituted derivatives (12-7NG-12, 12-7NK-12, 12-7NGK-12 and 12-7NKK-12), but all exhibited significantly higher gene expression compared to the parent compound, 12-7NH-12 of 168 ± 18 pg IFN-γ/2 × 10^5 cells ($p < 0.001$). As observed in earlier studies [5], the *in vitro* transfection efficiency of Lipofectamine in PAM 212 cells is higher compared to the gemini surfactants. Overall, gene expression in PAM212 was 1–6-fold higher compared to Sf 1Ep cells. In the Sf 1Ep cell line, the trend was similar to the COS7 cells, the 12-7NG-12 and 12-7NGK-12 PGLs showing higher gene expression at 72 h compared to the 12-7NK-12 and 12-7NKK-12 PLGs at 72 h. IFN-γ levels in the 12-7NG-12 PGL-transfected cells (329 ± 46 pg IFN-γ/2 × 10^5 cells) was significantly higher compared to all other delivery systems ($p < 0.001$). The transfection efficiency of the Lipofectamine was very low in the Sf 1Ep cells.

3.4. Physicochemical characterization of the amino acid/dipeptide-substituted gemini surfactant based transfection complexes

3.4.1. Size and zeta potential measurements

PGL complexes were prepared in a similar manner to those used for the transfection experiments. Particle sizes for all complexes were in the 110–140 nm range (Table 3). The plasmid/DOPE complexes showed slightly smaller particle size, slightly less than 100 nm. The zeta potential of −32.7 ± 0.6 mV of the plasmid/DOPE complexes shifted to +20–40 mV.

3.4.2. Circular dichroism

Circular dichroism was used to evaluate compaction of the DNA by the substituted gemini surfactants. Plasmid–gemini surfactant without DOPE and PGL complexes were prepared in a similar manner to those for the transfection experiments. The plasmid DNA alone showed two positive peaks at 295 and 255 nm, while all PG complexes had a blue shift of the 295 nm peak and depression of the 255-nm peak (Fig. 7A). The 12-7NG-12 PGL shows a flattening of the 295-nm peak, and the other compounds, including the parent 12-7NH-12 surfactant, show a slight depression (Fig. 7B). The pattern of the plasmid–DOPE mixture showed a positive peak at 275 nm.

4. Discussion

4.1. Characterization of the amino acid/dipeptide-substituted gemini surfactants

The specific conductivity plots are characteristic of gemini surfactants in general, with no evidence of pre-micelle aggregation. The observed break points are somewhat broader than that observed for the 12-7NH-12 2Br^- surfactant but more in line with that shown for the gemini 12-7NH-12 2Cl^- (Fig. 4). Note that these amino acid/peptide gemini surfactants have, in addition to the traditional two quaternary ammonium charged sites with Cl^- counterions, 1–3 primary amine sites that are in the form of HCl salts. The increase in the magnitude of the specific conductance for these compounds correlates well with the increase in number of the latter sites in the gemini surfactant. These spacer substituents are hydrophilic and make the spacer more hydrated than in the case of the 12-7NH-12 parent cation, and this is consistent with the order of the cmc values (Table 1); 12-7NKK-12 > 12-7NGK-12 > 12-7NK-12 > 12-7NG-12 > 12-7NH-12 and the broad break in the specific conductance lines of Fig. 4. Alternatively, the increased hydrophilicity of the head group will also likely result in a change in the micelle dynamics and may also be partially responsible for this observation.

The shape of the conductance profile, specifically the lack of a sharp break for 12-7NH-12, also suggests that there may be a difference in the dynamics of self-aggregation associated with the chloride when compared to the bromide counterion. Such an observation is not inconsistent with previous results for gemini surfactants where different counterions were found to produce different aggregation behaviour [19]; however, this feature requires additional study.

The aggregate sizes (Table 2) determined from DLS measurements show that they increase with the size of the amino acid/dipeptide substitution on the imino spacer of the gemini and their magnitude is approximately consistent with the expected overall length of a fully extended C12 alkyl tail, quaternary head group and extended amino acid. A decrease in the hydrodynamic diameters of the self-aggregates of these gemini compounds was found to occur as the post-micelle concentration was increased. Estimates of micelle counterion dissociation α (Table 1) measured near the cmc show that Cl^- is less tightly bound in the gemini surfactant with amino acid-substituted spacer than in the case of the parent compound, and this can lead to a higher surface charge density in the former aggregates. As the surfactant concentration is increased, growth of the aggregates must occur in a manner such as to minimize the repulsive forces in the head group region of the aggregates. This may be achieved by appropriate changes in the shape of the aggregates to overcome this stress. A change to a bilayer-like structure would be enhanced by favourable intermolecular hydrogen bonding between the keto-oxygen and the primary amine hydrogens of adjacent amino acids. This could lead to compaction of the aggregates as the amino acids become less extended from the aggregate surface. Thus, one might expect a transformation from a polydisperse to a less disperse distribution of

aggregates. High polydispersity index (PDI) values (ca. 1) were found for all amino acid/dipeptide spacer-substituted gemini at the lower concentration, i.e., nearer to the cmc. However, at the higher concentration, the PDI values decreased to 0.8 < PDI < 1.0 in several cases. The rather broad break points in the specific conductance graphs (Fig. 4) are also qualitatively consistent with the higher polydispersity of the aggregates as they form at the cmc; the *d* values from Eq. (1) (Table 1) indicate the width of the transition between the pre-micellar and post-micellar slopes and are indicative of this broadness.

4.2. In vitro transfection efficiency of the amino acid/dipeptide-substituted gemini compounds

We have studied the *in vitro* transfection efficiency of novel amino acid-substituted gemini surfactants in three different epithelial cell lines. The epithelial cell lines were used primarily to evaluate the performance of these compounds with potential application in scleroderma, atopic dermatitis and wound healing. Gemini surfactants self-assemble into higher order structures, and their aggregation depends on the length and chemical nature of the spacer [20] that also determines the fit between the positively charged nitrogens of the head group and the phosphate backbone of the DNA [21]. Previously, the transfection efficiency of the alkyl spacer gemini surfactants was found to vary inversely with their head group area determined from Gibbs interfacial energy [5]. Imino substitution in the spacer introduced a better fit with the DNA and conferred pH sensitivity to the gemini surfactants [8], which could reduce cytotoxicity and facilitate endosomal escape of the DNA. Polylysine and polyallylamine showed relatively high cytotoxicity due to their polycationic nature and the presence of primary amine groups. Substitution of the primary amines with imidazoyl derivatives not only reduced cytotoxicity, but also improved endosomal escape of the genetic material [22]. The amino acid-substituted gemini surfactants show higher gene expression compared to the unsubstituted parent compound 12-7NH-12 in all three cell lines (Figs. 5 and 6) investigated in this work. Cationic agents non-specifically bind the cell surface through ionic interactions with membrane-associated proteoglycans [23]. Differences in the gene expression among the three cell lines might be due to the differences in the distribution of proteoglycans on the cell surface. Transgene expression depends not only on compaction by the cationic agent and delivery of the genetic material into the cells but also on endosomal escape and release of the DNA from the complexes. It appears that grafting of amino acids or peptides on the gemini surfactant molecule can improve the delivery and release of the DNA in the cytoplasm. It should be noted that a weak binding in the PG complex does not protect and compact sufficiently, whereas strong binding will not allow for the release of the DNA. While gemini surfactants bind the DNA via electrostatic interactions, the nature of binding by the amino acid and peptide-substituted gemini surfactants might be 'softened' by van der Waals and hydrogen bonding forces [24], thus increasing the flexibility and plasticity of the supramolecular structures [25]. Increased hydrophilicity of the amino acid-substituted gemini surfactants compared to the parent compound might translate into better biocompatibility. The increased biocompatibility of these peptidomimetic particles could lead to lower cytotoxicity. The gene expression pattern showed similarities with higher gene expression in the cells transfected with glycine-substituted and glycyl-lysine substituted gemini surfactants. Although it was expected that the substituted gemini surfactants would form larger complexes due to a larger hydrophilic head, there was no significant difference compared to the parent compound (Table 3). Complex sizes of 100–150 nm are optimal for endocytotic internalization by the cells [26]. Zeta potential of the particles is approximately +30 mV for all compounds, which indicates that the system is colloidally stable [27]. There was no difference between the zeta potential of the unsubstituted 12-7NH-12 and amino acid/dipeptide-substituted gemini surfactants, indicating that substitution did not shield the surface charge on the particles. The CD spectra obtained are consistent with those previously reported for gemini surfactants [8,13,28]. Previously, such changes in the native DNA structure were interpreted in terms of the surfactants inducing formation of Ψ^- DNA [29], which usually required high salt concentrations. The changes observed for the gemini surfactants are more consistent with a B-DNA conformation in which both the helicity and base stacking are perturbed as a result of compaction of the DNA molecule by the surfactant [30]. The similarity between the profiles obtained for the amino acid-substituted vs. unsubstituted gemini surfactants (Fig. 7) indicates that the substitution on the spaced does not interfere with the ability of the gemini surfactant to compact DNA.

5. Conclusion

Amino acid and peptide-substituted imino spacer of gemini surfactants transfect epithelial cells at higher efficiency compared to unsubstituted imino spacers. The substitution does not increase the size of the particles or reduce zeta potential, nor weaken DNA compaction. The higher transfection efficiency is attributed to the higher biocompatibility and flexibility of the amino acid/peptide-substituted gemini surfactants and demonstrates the feasibility of using amino acid-substituted gemini surfactants as gene carriers for the treatment of diseases affecting epithelial tissue.

Acknowledgements

The authors thank the Saskatchewan Structural Sciences Centre (SSSC) for the use of NMR, ESI-MS and CD instruments and Mr. Jason Maley for analysis and discussions. Financial assistance provided to R.E.V. by the Natural Science and Engineering Research Council of Canada (NSERC) is gratefully acknowledged.

References

[1] B. Freundlich, S.A. Jimenez, V.D. Steen, T.A. Medsger Jr., M. Szkolnicki, H.S. Jaffe, Treatment of systemic sclerosis with recombinant interferon-gamma. A phase i/ii clinical trial, Arthritis Rheum. 35 (1992) 1134–1142.
[2] L.M. Buys, Treatment options for atopic dermatitis, Am. Fam. Physician 75 (2007) 523–528.
[3] H. Emmez, O. Kardes, F. Dogulu, G. Kurt, L. Memis, M.K. Baykaner, Role of antifibrotic cytokine interferon-gamma in the prevention of postlaminectomy peridural fibrosis in rats, Neurosurgery 62 (2008) 1351–1357 (discussion 7–8).
[4] F.M. Menger, J.S. Keiper, Gemini surfactants, Angew. Chem. Int. Ed. Engl. 39 (2000) 1906–1920.
[5] I. Badea, R. Verrall, M. Baca-Estrada, et al., In vivo cutaneous interferon-gamma gene delivery using novel dicationic (gemini) surfactant-plasmid complexes, J. Gene Med. 7 (2005) 1200–1214.
[6] M.L. Fielden, C. Perrin, A. Kremer, et al., Sugar-based tertiary amino gemini surfactants with a vesicle-to-micelle transition in the endosomal ph range mediate efficient transfection in vitro, Eur. J. Biochem. 268 (2001) 1269–1279.
[7] H.S. Rosenzweig, V.A. Rakhmanova, R.C. MacDonald, Diquaternary ammonium compounds as transfection agents, Bioconjugate Chem. 12 (2001) 258–263.
[8] S.D. Wettig, I. Badea, M. Donkuru, R.E. Verrall, M. Foldvari, Structural and transfection properties of amine-substituted gemini surfactant-based nanoparticles, J. Gene Med. 9 (2007) 649–658.
[9] E. Fisicaro, C. Compari, E. Duce, G. Donofrio, B. Rozycka-Roszak, E. Wozniak, Biologically active bisquaternary ammonium chlorides: physico-chemical properties of long chain amphiphiles and their evaluation as non-viral vectors for gene delivery, Biochim. Biophys. Acta 1722 (2005) 224–233.
[10] R. Zana, Dimeric (gemini) surfactants: effect of the spacer group on the association behavior in aqueous solution, J. Colloid Interf. Sci. 248 (2002) 203–220.
[11] L. Karlsson, M. van Eijk, O. Soderman, Compaction of DNA by gemini surfactants: effects of surfactant architecture, J. Colloid Interf. Sci. 252 (2002) 290–296.

[12] C. Wang, X. Li, S.D. Wettig, I. Badea, M. Foldvari, R.E. Verrall, Investigation of complexes formed by interaction of cationic gemini surfactants with deoxyribonucleic acid, Phys. Chem. Chem. Phys. 9 (2007) 1616–1628.
[13] M. Foldvari, I. Badea, S. Wettig, R. Verrall, M. Bagonluri, Structural characterization of novel gemini non-viral DNA delivery systems for cutaneous gene therapy, J. Exp. Nanosci. 1 (2006) 165–176.
[14] R. Kharidia, K.A. Friedman, J.F. Liang, Improved gene expression using low molecular weight peptides produced from protamine sulfate, Biochemistry (Mosc.) 73 (2008) 1162–1168.
[15] S.D. Wettig, R.E. Verrall, Thermodynamic studies of aqueous m–s–m gemini surfactant systems, J. Colloid Interf. Sci. 235 (2001) 310–316.
[16] T.Y. Zakharian, A. Seryshev, B. Sitharaman, B.E. Gilbert, V. Knight, L.J. Wilson, A fullerene-paclitaxel chemotherapeutic: synthesis, characterization, and study of biological activity in tissue culture, J. Am. Chem. Soc. 127 (2005) 12508–12509.
[17] X. Li, S.D. Wettig, C. Wang, M. Foldvari, R.E. Verrall, Synthesis and solution properties of gemini surfactants containing oleyl chains, Phys. Chem. Chem. Phys. 7 (2005) 3172–3178.
[18] P. Carpena, J. Aguiar, P. Bernaola-Galvan, C.C. Ruiz, Problems associated with the treatment of conductivity–concentration data in surfactant solutions: simulations and experiments, Langmuir 18 (2002) 6054–6058.
[19] N. Jiang, P.X. Li, Y.L. Wang, J.B. Wang, H.K. Yan, R.K. Thomas, Aggregation behavior of hexadecyltrimethylammonium surfactants with various counterions in aqueous solution, J. Colloid Interf. Sci. 286 (2005) 755–760.
[20] E. Alami, G. Beinert, P. Marie, R. Zana, Alkanediyl-alpha, omega-bis(dimethylalkylammonium bromide) surfactants. 3. Behavior at the air–water-interface, Langmuir 9 (1993) 1465–1467.
[21] X. Chen, J. Wang, N. Shen, et al., Gemini surfactant/DNA complex monolayers at the air–water interface: effect of surfactant structure on the assembly, stability, and topography of monolayers, Langmuir 18 (2002) 6222–6228.
[22] A. Pathak, A. Aggarwal, R.K. Kurupati, et al., Engineered polyallylamine nanoparticles for efficient in vitro transfection, Pharm. Res. 24 (2007) 1427–1440.
[23] K.A. Mislick, J.D. Baldeschwieler, Evidence for the role of proteoglycans in cation-mediated gene transfer, Proc. Natl. Acad. Sci. USA 93 (1996) 12349–12354.
[24] E. Jabbari, Targeted delivery with peptidomimetic conjugated self-assembled nanoparticles, Pharm. Res. 26 (2009) 612–630.
[25] G. Colombo, P. Soto, E. Gazit, Peptide self-assembly at the nanoscale: a challenging target for computational and experimental biotechnology, Trends Biotechnol. 25 (2007) 211–218.
[26] M.R. Almofti, H. Harashima, Y. Shinohara, A. Almofti, Y. Baba, H. Kiwada, Cationic liposome-mediated gene delivery: biophysical study and mechanism of internalization, Arch. Biochem. Biophys. 410 (2003) 246–253.
[27] W. Mehnert, K. Mader, Solid lipid nanoparticles: production, characterization and applications, Adv. Drug Deliv. Rev. 47 (2001) 165–196.
[28] I. Badea, S. Wettig, R. Verrall, M. Foldvari, Topical non-invasive gene delivery using gemini nanoparticles in interferon-gamma-deficient mice, Eur. J. Pharm. Biopharm. 65 (2007) 414–422.
[29] D. Simberg, D. Danino, Y. Talmon, et al., Phase behavior, DNA ordering, and size instability of cationic lipoplexes. Relevance to optimal transfection activity, J. Biol. Chem. 276 (2001) 47453–47459.
[30] C.S. Braun, G.S. Jas, S. Choosakoonkriang, G.S. Koe, J.G. Smith, C.R. Middaugh, The structure of DNA within cationic lipid/DNA complexes, Biophys. J. 84 (2003) 1114–1123.